Langmuir

Article

pubs.acs.org/Langmuir

Nanomechanical Actuation of a Silicon Cantilever Using an Azo Dye, Self-Assembled Monolayer

A. Joseph Rastegar,[†] Michael Vosgueritchian,[‡] Joseph C. Doll,[†] Joseph R. Mallon,[†] and Beth L. Pruitt*[,†]

[†]Department of Mechanical Engineering and [‡]Department of Chemical Engineering, Stanford University, Stanford, California 94305

ABSTRACT: The emerging fields of nanomotors and optomechanics are based on the harnessing of light to generate force. However, our ability to detect small surface stresses is limited by temperature drift, environmental noise, and low-frequency flicker electronic noise. To address these limitations, we functionalized microfabricated silicon cantilevers with an azo dye, silane-based self-assembled monolayer and modulated the surface stress by exciting the optical switch with a 405-nm laser. Atomic force microscopy, contact angle analysis, ellipsometry, and X-ray photoelectron spectroscopy verified successful assembly of molecules on the cantilever. Ultraviolet and visible spectra demonstrate optical switching of the synthesized molecule in solution. By turning the laser on and off at a specific rate (e.g., 1 Hz), the cantilever deflection can be measured via Fourier techniques, thus separating the signal of interest from the noise. This technique empowers the design of highly sensitive surface stress measurements.

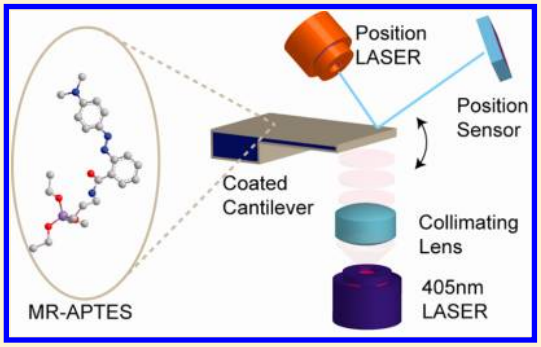

INTRODUCTION

Silicon micromachined cantilevers are used for measuring small forces in atomic force microscopy (AFM),[1] and in the last two decades, silicon cantilevers have also been used as surface stress sensors.[2] Cantilevers can form the basis of chemically specific sensors by coupling molecular recognition agents to the cantilever surface.[3] Upon binding of the analyte to the surface receptor, a surface stress is induced[4] due to the electronic structure of the surface,[5,6] conformation changes caused by analyte-receptor binding, surface polarity, and surface interactions with the solvent. Importantly, only one surface of the cantilever must be functionalized because functionalization of both surfaces would result in equal stresses on both sides, and no tip deflection would occur.

To construct a differential surface, gold is usually deposited on one side of the cantilever and thiol chemistry is used for the attachment of the desired layer.[7] However, the large coefficient of thermal expansion mismatch between gold and silicon renders the cantilever very sensitive to temperature variations,[8] reducing long-term measurement resolution. Other sources of low-frequency noise include environmental noise, such as humidity fluctuations, and flicker noise in the signal conditioning electronics. Gold grain size and deposition conditions also have major impacts on the repeatability and reproducibility of results.[9] In a seminal work, Godin[10] showed that for gold-coated cantilevers functionalized with alkanethiols, the gold−sulfur bond generates 6 N/m of surface stress independent of the alkane chain length. This large surface stress was attributed to surface charge redistribution that led to the rearrangement of the gold surface atoms. Alkane chains or vertical interactions,[11] which are the main components of biomolecular forces, only generate surface stresses on the order of 1 mN/m. Hence, gold-coated cantilevers need to operate at the lower end of their sensitivity in the presence of large common-mode error.

We propose to eliminate gold from the system and instead to use single-crystal silicon with native oxide cantilevers with repeatable properties and to modulate the cantilever surface-stress signal over time using light and an azo dye. This design spectrally separates the sensor signal from the background noise to achieve differential top and bottom surfaces on the same cantilever.[12] The light is shone on one side of the cantilever, while both sides are coated with an azobenzene derivative. The physical behaviors of azo dyes are based on the isomerization of constituent molecules, which undergo a large conformational change from one state to another in response to the absorption of light at distinct wavelengths.[13] The light-induced transition of azobenzene derivatives ($C_6H_5N{=}NC_6H_5$) between the extended (trans) and compact (cis) configurations gives rise to changes in molecular polarity, dipole moment, and shape. Most azobenzene-based thin films are fabricated into materials such as polymers, liquid crystals, Langmuir−Blodgett films,[14] and physically or chemically adsorbed monolayers on gold surfaces.[15−19] In practice, photoswitches are strongly influenced by the density and orientation of azobenzene-based self-assembled monolayers (SAMs). For example, an azobenzene-contained alkanethiol self-assembled onto gold substrates exhibited no response upon UV irradiation due to steric hindrance.[20,21] The minimum area for isomerization of azobenzene has been estimated as 0.4 nm^2.[22] In contrast to thiol-based SAMs, specific silane-based SAMs provide sufficient room between molecules to prevent

Received: June 19, 2012
Revised: May 8, 2013
Published: May 10, 2013

dx.doi.org/10.1021/la3034676 | *Langmuir* 2013, 29, 7118−7124

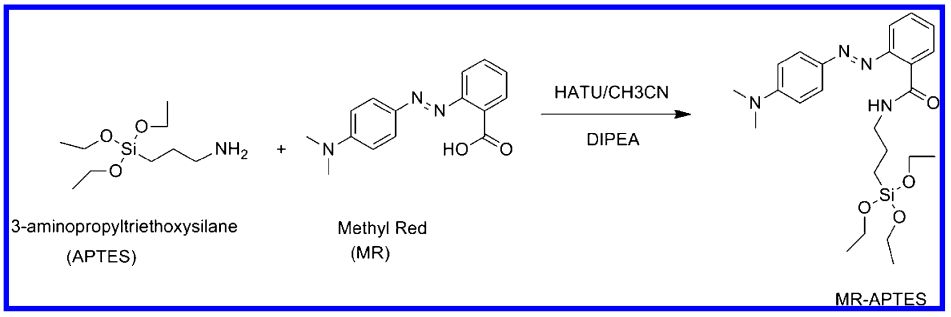

Figure 1. Chemical synthesis of MR-APTES. APTES and MR precursors are combined in room-temperature acetonitrile and the formation of an amine-based linkage is catalyzed by HATU to form MR-APTES. Synthesis is fast, specific, and requires a single step and container.

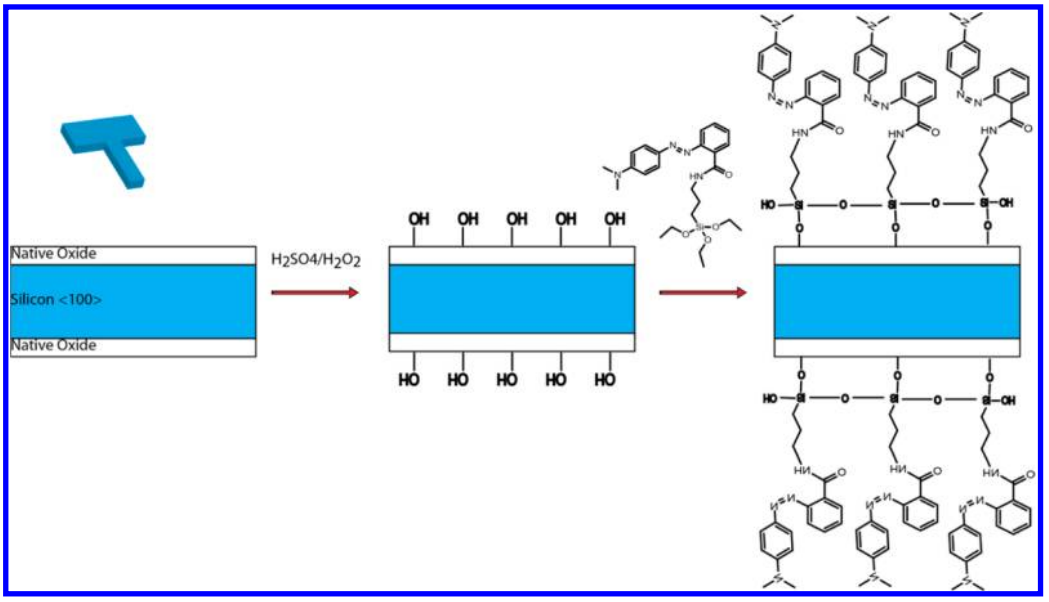

Figure 2. Process flow of cantilever functionalization. The silicon microcantilevers are first hydroxylated in piranha solution and then functionalized with MR-APTES.

steric hindrance and have been shown to serve as alignment layers for liquid crystal networks.[23,24]

Surfaces functionalized with light-responsive materials provide the unique capability of exploiting different surface stresses depending on the light shone on the surface. By selecting molecules that can be reversibly photoisomerized at a specific rate (e.g., 1 Hz), we improved the signal-to noise-ratio via Fourier techniques. Here, we demonstrate that an (*E*)-2-((4-(dimethylamino)phenyl)diazenyl)-*N*-(3(triethoxysilyl)-propyl)benzamide (MR-APTES) SAM can be reversibly switched using a 405-nm laser, enabling surface-stress modulation of a silicon microcantilever. Methyl red (MR) served as the functional group and APTES provided the attachment to the silicon substrate. We hypothesize that the observed photoswitching effect is due to the isomerization of the molecule, which converts the optical energy at a specific wavelength to mechanical motion. This effect may empower the design of next-generation chemical sensors, nanomotors, and highly efficient solar cells.[25]

EXPERIMENTAL SECTION

Synthesis of MR-APTES. MR-APTES was synthesized at room temperature in a nitrogen atmosphere. All precursor chemicals were purchased from Sigma Aldrich and used as received. 3-Aminopropyltriethoxy silane (1.55 g, 7.0 mmol) was added to a solution of MR (1.88 g, 7.0 mmol) in acetonitrile (35 mL). The resulting red solution was treated with diisopropylethylamine (DIPEA) (1.35 g, 10.5 mmol) followed by portion-wise addition of *N*-[(dimethylamino)-1*H*-1,2,3-triazolo[4,5-*b*]pyridinylmethylene)-*N*-methylmethanaminium hexafluorophosphate *N*-oxide] (HATU; 3.99 g, 10.5 mmol; Figure 1). HATU is an efficient, fast, and specific activating agent for amine-based molecular coupling.[26] The reaction mixture was stirred for 8 h. The solvent was removed under reduced pressure, and the product was purified by flash column chromatography over silica gel using 35% ethyl acetate/hexane to 50% ethyl acetate/hexane to yield 1.85 g of MR-APTES as a red solid (56% yield). We used MedChem LLP for recurring synthesis of MR-APTES (www.medchemsource.com).

Monolayer Preparation. To prepare the monolayer, we made a 20 mM solution of MR-APTES in anhydrous toluene. We ensured the use of dry glassware and dry solvent since water catalyzes the polymerization of APTES. Our protocol achieved acceptable yield with azobenzoic and benzoic acid, whereas the molecules polymerized in solution when coupled to 3-aminopropyltrimethoxy silane, which is more reactive with water.[27]

Cantilevers were placed in room-temperature piranha solution (4:1 H_2SO_4:30% H_2O_2) for 5 min to clean and hydroxylate the surface. The cantilevers were then thoroughly rinsed with deionized water, sonicated for 30 s in deionized water, and rinsed again with high-purity deionized water (18 MOhm; Millipore). The water contact angle is approximately zero at this step if the surface is properly hydroxylated.[28]

For functionalization (Figure 2), the cantilevers were dried for 10 min and placed in a glass vial of 20 mM MR-APTES in anhydrous

dx.doi.org/10.1021/la3034676 | *Langmuir* 2013, 29, 7118−7124

toluene. The vial was purged with nitrogen, and the lid was closed for 2 h at room temperature. Care was taken to keep water out of the reaction because water catalyzes the attachment of ethoxy silane to the hydroxylated silicon dioxide surface; excess water thus causes the silane to polymerize on the surface. After 2 h, the cantilevers were removed, rinsed with pure toluene, and sonicated for 10 s in ethanol.

Characterization of the MR-APTES Monolayer. Contact angle, AFM, ellipsometry, XPS, and optomechanical modulation of the surface stress were used to characterize the MR-APTES monolayer. Due to the small size of the cantilever and associated handling issues, these analyses were performed on ∼1 × 1 cm pieces of silicon that were processed with cantilevers at the same time and under the same conditions. The measurements of contact angle, AFM, and XPS of the 1 ×1 cm pieces of silicon were similar to the measurements from broken cantilevers.

Single-crystal silicon microcantilevers were purchased from Nanoworld and were 1-μm thick, 100-μm wide, and 500-μm long. The gold-coated cantilevers used for thermal characterization were also of the same dimension and made of single crystal silicon with 25 nm of Au and 5 nm Cr adhesion deposited on the top side.

The two lasers used (405 nm, 635 nm) were both purchased from THORLABS. They were Fiber-pigtail lasers (LP405, LP635) and were used with an appropriate collimator. The laser power was adjusted by measuring the current through the laser diode and using the manufacturer data sheet to convert current to light output power. The measurements were confirmed additionally against a THORLABS PM10 sensor and laser power meter placed at the cantilever location.

Water contact angle measurements were taken with an FTA 1000 Goniometer (First Ten Angstroms). AFM images were taken in tapping mode (light tapping regime) using a Multimode AFM (Veeco). We used a Nanofilm EP3 532 nm variable angle ellipsometer to measure film thickness. We assumed the refractive index of the MR-APTES to be n = 1.6, which is the average value of the MR and APTES refractive indices (the MR:APTES ratio is 1:1). The absorbance was assumed to be k = 1.8 and dominated by MR, since APTES is transparent (the manufacturer's stated k value is zero). The values used were taken from the bulk measurements of Taqatqa et al.[29] The thickness of the native oxide underlying the MR-APTES film was measured as 2.1 nm.[30]

X-ray photoelectron spectroscopy (XPS) was performed on an SSI S-Probe monochromatized X-ray photoelectron spectrometer system, with an Al ($K\alpha$) X-ray source (1486.6 eV) in a UHV system with a base pressure in the 10^{-9} Torr range. The survey scans were collected by using a hemispherical electron energy analyzer at a pass energy of 156.5 eV with 1-eV resolution. The XPS data were processed by Shirley background correction followed by fitting to Voigt profiles. A bulk C(1s) peak at 284.6 eV was used to adjust all of the peaks to correct the binding energies for the charge shift.[31]

Electronic absorption spectra were recorded on a SHIMADZU UV-1800 spectrophotometer. Optical-mechanical modulation experiments were performed using a Witec Alpha300 atomic force microscope. The displacement sensitivity of the AFM system was measured by indenting a glass slide; the spring constants of the cantilevers were calibrated from the thermomechanical noise.[32]

RESULTS AND DISCUSSION

We first observed the absorption spectra of a toluene solution of MR-APTES to verify that the attachment of APTES to MR did not prevent photoisomerization of the molecule in solution, as observed by a reversible absorbance change in MR-APTES (Figure 3). We were concerned that the bulky alkyl chain may prevent isomerization. Because silicon is opaque in the visible and UV ranges of the spectrum, measurement of the absorption change that would demonstrate isomerization of a monolayer was not possible, as Yi et al.[24] showed on glass slides.

The absorption spectra of MR-APTES in toluene were determined with various times of exposure to a 405-nm laser (Figure 3), and the resulting classic photochromisim indicated a

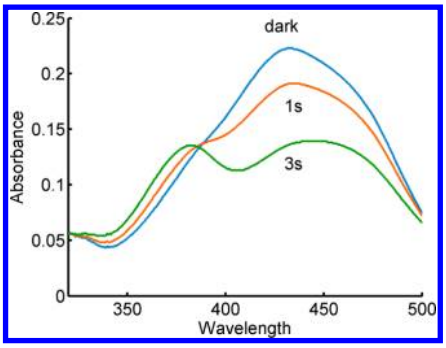

Figure 3. Absorbance spectra of MR-APTES in toluene. A 10-μM solution of MR-APTES was placed in a quartz cuvette, kept in the dark, and the absorbance was recorded. The solution was then exposed to 405-nm light for 1 and 3 s to demonstrate photochromism.[35] The absorbance recovered when left in the dark to its original absorbance (data not shown for clarity).

trans−cis change in the population of the molecules. The time required for cis−trans thermal isomerization can range from hours/days (azobenzenes) to milliseconds (aminoazobenzenes).[33] Photoisomerization can be viewed as photochemical reaction that reaches equilibrium. Azobenzene species adopt a photostationary state in which equilibrium is reached through the process of light-driven trans−cis and cis−trans isomerization, as well as thermally driven cis−trans isomerization. The energy of the trans form of azobenzenes is 50 kJ/mol less than that of the cis form, making the trans form stable in the dark.[34] The ortho- or para-substitution of an azobenzene ring with an amine group yields an aminoazobenzene such as MR, in which the n−π^* and π−π^* bands are overlapping in the violet due to an increase in the π orbital energy and a decrease in the energy of the π^* orbital.[12,35]

Surface properties of MR-APTES were investigated by sessile drop contact angle analysis (Figure 4, left) and AFM (Figure 4, right). For a typical SiO_2 surface, the contact angle is less than 30°;[36] however, our MR-APTES SAM exhibited repeatable water contact angles of 70° ± 2° over six different areas. Contact angle measurements are influenced by surface topography, and thus AFM was used to evaluate surface roughness and the existence of aberrant surface particles. The surface roughness of the monolayer was 0.2 nm RMS (Figure 4, right), indicative of a continuous, high-quality monolayer film without island growth or particles.

We measured the thickness of the MR-APTES film as approximately 1 nm via variable angle ellipsometry. XPS revealed no carbon or nitrogen signals in the piranha-cleaned silicon (Figure 5); however, the MR-APTES-coated cantilever exhibited carbon and nitrogen peaks at a ratio of 6.4:1, which is close to the expected value of 6:1.

Optomechanical modulation of the cantilever was measured using the optical beam bounce method (Figure 6). A 405-nm solid-state laser was placed beneath the cantilever, and the illumination intensity was set by a custom-made laser driver. The on−off time of the laser was set by a waveform generator. The cantilever was placed on a glass slide (Corning 2947) in air. When the MR-APTES-coated cantilever was exposed to the 405-nm laser from the bottom, the tip deflected upward, and when the 405-nm laser was turned off, the tip deflected downward.

In a seminal work, Yi et al.[37] showed that MR-APTES on glass slide has a relaxation time of ∼560 s. Their measurements

dx.doi.org/10.1021/la3034676 | Langmuir 2013, 29, 7118−7124

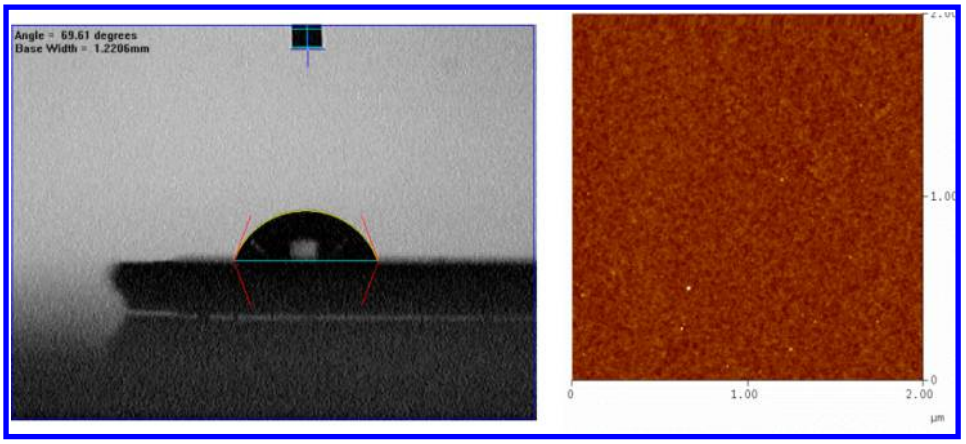

Figure 4. The contact angle of the surface (left), and the AFM of the surface (right) with a height scale of 10 nm. The contact angle of six spots from three samples was 70° ± 2°, and the surface roughness was approximately 0.2 nm RMS for a 2 × 2 μm area.

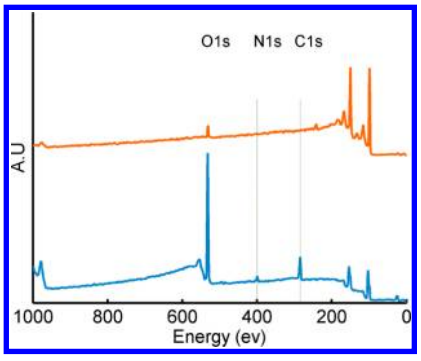

Figure 5. XPS measurements verify the successful functionalization of silicon with MR-APTES. A significant ratio of carbon to nitrogen (6.4) is present on the MR-APTES functionalized silicon (blue) but absent from the bare silicon (orange).

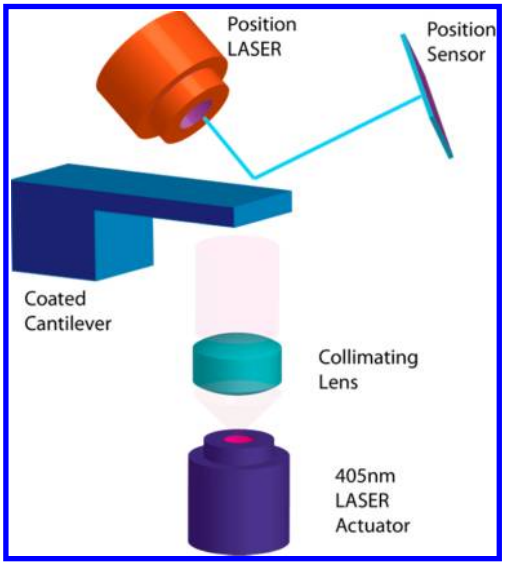

Figure 6. Experimental setup for optomechanical modulation. The MR-APTES-coated cantilever is optomechanically actuated using a 405-nm laser. The tip deflection of the cantilever is recorded using the optical beam bounce technique.

were based on the absorbance of a monolayer of MR-APTES on glass; similar measurements on silicon are not possible because silicon is opaque, hindering our ability to estimate the bias of the photostationary state. The thermal relaxation time of MR-APTES in chloroform solution reported by Yi et al.[37] is 0.7 s. The difference between the solution and monolayer thermal relaxation times was hypothesized to be due to molecular spacing. The molecules are separated by ∼25 nm in solution and ∼0.7 nm in a monolayer.[37] A hallmark of Yi's thermal relaxation time is its exponential nature. A different model that more closely matches our data is based on the work of Fang et al.,[38] who described a faster relaxation time due to softening of the monolayer by athermal photofluidization. Although the mechanisms of actuation are not completely clear at the moment, it is clear that the MR-APTES molecule causes the motion of the cantilever in our system.

There are fundamental differences between our system and the systems of Yi et al. and Fang et al. The main differences are in the nature of the oxide, the rigidity of the substrate, and the measurements of absorbance and birefringence instead of direct mechanical motion. The surface and composition of glass can significantly differ from those of a silicon dioxide surface. Rigidity of the substrate is another major difference; here we used soft ∼1 μm-thick cantilevers with a spring constant of ∼30 mN/m.

Substantial noise and drift were detected in the raw deflection of the cantilever beam due to its low spring constant of 30 mN/m (Figure 7, left). However, the noise was minimized by averaging the cantilever motion on a cycle-by-cycle basis (Figure 7, right). The deflection spectra of an uncoated reference cantilever and MR-APTES coated cantilever are presented in Figure 8; deflection of the coated cantilever was 1 order of magnitude greater than the reference cantilever at the laser modulation frequency (1 Hz) and exhibited large, even harmonics in contrast.

To further investigate the tip movement, we used a laser with a wavelength at which MR-APTES does not isomerize (635 nm; Figure 9). At both wavelengths, most of the heat generated was due to the absorption of photons by the silicon cantilever rather than by the monolayer. Yi et al.[24] reported an absorbance of 8×10^{-3} for two MR-APTES monolayer (both side of glass slide) at a maximum absorbance wavelength of 435 nm. Therefore, most of the light is transmitted through the MR-APTES into the silicon. The absorption coefficient of silicon is 1.0×10^{7}/m and 3.5×10^{5}/m at 405 and 635 nm, respectively;[39] therefore, the incident light is efficiently absorbed by the 1-μm thick cantilever beam in both cases. When we varied the laser power at 405 nm from 1 mW to 8 mW, we observed a linear increase in the amplitude of

dx.doi.org/10.1021/la3034676 | *Langmuir* 2013, 29, 7118−7124

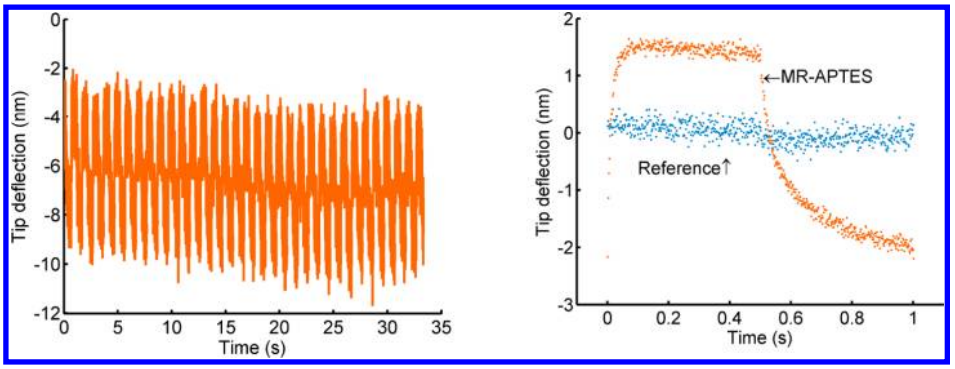

Figure 7. Optomechanical motion of the cantilever. Left, raw output of the AFM tip deflection for an MR-APTES-coated cantilever. Right, mean corrected cycle average of 119 pulses of the MR-APTES (orange) and the reference cantilever (blue). The uncoated reference cantilever does not show motion, while the MR-APTES coated cantilever does. One-hundred nineteen pulses were averaged to improve the signal-to-noise ratio. The turn-on time is substantially faster than the turn-off time due to the finite rate of cis−trans thermal isomerization.

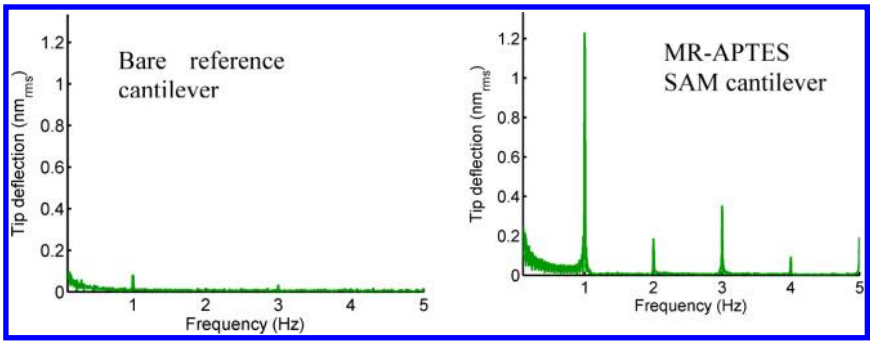

Figure 8. MR-APTES enables optomechanical actuation of microcantilevers. When a bare silicon reference cantilever (left) is excited with a 405-nm laser at 1 Hz, a small peak appears at the modulation frequency and even harmonics are not visible. The deflection amplitude of a cantilever functionalized with MR-APTES (right) increases 10-fold at the modulation frequency and even harmonics are visible in the spectrum due to the difference in the on- and off-rates of actuation.

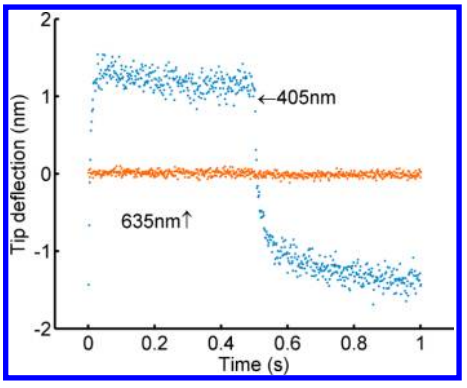

Figure 9. An MR-APTES-coated cantilever exhibits actuation when excited with 405-nm laser, and no actuation when excited with a 635-nm laser. The laser power was approximately 2 mW for both wavelengths. The wavelength specificity is consistent with an optomechanical rather than thermal actuation mechanism.

deflection and did not observe any discernible response at 635 nm when the power was varied.

By observing tip deflection in the frequency domain, it is possible to gain more insight about the signal. For example, in the cycle average of the reference cantilever, the tip deflection at 1 Hz was obscured by noise, but we detect a small peak in the frequency domain with the functionalized cantilever. A perfectly symmetrical square wave in which the on and off times are identical shows only odd harmonics, which can be mathematically shown by Fourier analysis. For the gold-coated and reference cantilevers, we only observe odd harmonics that are related to the equal on and off times. As expected, the heating (light on) and cooling (light off) mechanisms are symmetric. In the case of MR-APTES, the photostationary states are reached faster during illumination than when the molecule is allowed to reach a stationary state in the dark. Therefore, the on and off times are asymmetric even though the input is symmetric, an effect that appears as even harmonics in the Fourier spectrum. In summary, the presence of even harmonics suggests asymmetry between the on- and off-times of the cantilever: thermal actuation is symmetric, while optomechanical actuation is not. This difference is due to the MR-APTES SAM.

To investigate the effects of cantilever heating, we used gold- and 11-Bromouncyltrimethoxysilane-coated cantilevers. Figure 10 shows tip deflection of a gold-coated cantilever excited with less than 100 μW laser power. The 1-μm thick silicon layer of the gold-coated cantilever absorbs the transmitted light and converts it to heat. The thermal coefficient of expansion of silicon[40] is 2.6 ppm/K, and the coefficient for gold is 14 ppm/K.[41] Because the metal is only deposited on the top of the cantilever, the heat expands the metal and the cantilever bends downward to accommodate this expansion.

While we would have preferred to test a monolayer with the same molar extinction coefficient as MR-APTES that does not isomerize, we were not able to obtain such a molecule. Therefore, we tested several different SAMs. APTES alone did not generate a monolayer following variants of our protocol, an effect that we attribute to the NH_2 group.[42] However, we

dx.doi.org/10.1021/la3034676 | Langmuir 2013, 29, 7118−7124

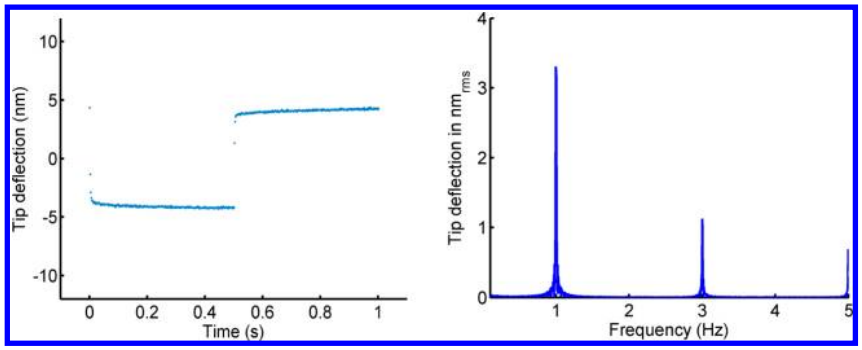

Figure 10. Time (left) and frequency domain (right) of the tip deflection of a gold-coated cantilever. The silicon−gold bimorph structure deflects due to the temperature increase induced by the incident optical power (<100 μW). Even harmonics are not present in the signal because the heating and cooling rates are the same. One-hundred nineteen pulses were averaged.

successfully coated cantilevers with 11-bromoundecyltrimethoxysilane. These cantilevers did not actuate. We observed a small tip deflection at the laser modulation frequency and the deflection only exhibited odd harmonics at 2 mW of laser power. This reproducible and repeatable monolayer had the same deposition condition as that of MR-APTES.

Each cantilever was individually calibrated, since the detector output of the AFM only provides a voltage, a sensitivity constant is needed to convert the voltage to the actual tip displacement. The width and length of the cantilevers are large; however, the thickness is small in comparison and subject to significant process variation. We measured the resonance frequency of each cantilever, and from the measured resonance frequency and measured thermomechanical noise at resonance, estimated the cantilever thickness and sensitivity.[32] We also verified the sensitivity against force displacement measurement on several cantilevers. Unfortunately, the force displacement method requires cantilever contact with a surface that can cause damage to the coating. Thus we rely primarily on the thermomechanical noise based calibration method. The deflection of the MR-APTES cantilever was equivalent to a surface stress change of 0.43 mN/m, corresponding to an average force on the order of 0.3 pN per molecule. The surface stress calculation was based on thermomechanical noise calibration of the cantilever, the application of Stoney's equation,[43] (where E_{110} = 168G Pa, Poisson's ratio = 0.28)[44] and an average molecular distance of 7 Å.

CONCLUSIONS

We have demonstrated that a monolayer of the amino-azobenzene MR-APTES physically exerts a surface stress due to absorbance of a 405-nm photon, resulting in the deflection of the tip of a micromachined cantilever. Since the surface stress can be repeatedly induced, averaging and Fourier techniques can be used for signal processing. The optomechanical modulation of surface stress should enable the spectral separation of the signal of interest from background noise sources in fundamental surface studies, enabling a new generation of surface stress-based sensing with improved signal-to-noise ratio.

AUTHOR INFORMATION

Corresponding Author

*E-mail: pruitt@stanford.edu.

Notes

The authors declare no competing financial interest.

ACKNOWLEDGMENTS

This work was supported by DARPA Grant (N66001-09-1-2089) and COINS Grant (ECCS-0832819). The authors are grateful to professors Curt Frank, Alex Dunn, and Gerard Marriott for helpful discussions.

REFERENCES

(1) Binnig, G.; Quate, C. F.; Gerber, C. Atomic Force Microscope. *Phys. Rev. Lett.* **1986**, *56*, 930−933.
(2) Ziegler, C. Cantilever-Based Biosensors. *Anal. Bioanal. Chem.* **2004**, *379*, 946−959.
(3) Fritz, J.; Baller, M. K.; Lang, H. P.; Strunz, T.; Meyer, E.; Guntherodt, H. J.; Delamarche, E.; Gerber, C.; Gimzewski, J. K. Stress at the Solid−Liquid Interface of Self-Assembled Monolayers on Gold Investigated with a Nanomechanical Sensor. *Langmuir* **2000**, *16*, 9694−9696.
(4) Fritz, J. Translating Biomolecular Recognition into Nanomechanics. *Science* **2000**, *288*, 316−318.
(5) Haiss, W. Surface Stress of Clean and Adsorbate-Covered Solids. *Rep. Prog. Phys.* **2001**, *64*, 591−648.
(6) Ibach, H. The Role of Surface Stress in Reconstruction, Epitaxial Growth and Stabilization of Mesoscopic Structures. *Surf. Sci. Rep.* **1997**, *29*, 195−263.
(7) Ramírez, E. A.; Cortés, E.; Rubert, A. A.; Carro, P.; Benítez, G.; Vela, M. E.; Salvarezza, R. C. Complex Surface Chemistry of 4-Mercaptopyridine Self-Assembled Monolayers on Au(111). *Langmuir* **2012**, *28*, 6839−6847.
(8) Loui, A.; Elhadj, S.; Sirbuly, D. J.; McCall, S. K.; Hart, B. R.; Ratto, T. V. An Analytic Model of Thermal Drift in Piezoresistive Microcantilever Sensors. *J. Appl. Phys.* **2010**, *107*, 054508−054521.
(9) Mertens, J.; Calleja, M.; Ramos, D.; Taryn, A.; Tamayo, J. Role of the Gold Film Nanostructure on the Nanomechanical Response of Microcantilever Sensors. *J. Appl. Phys.* **2007**, *101*, 034904−8.
(10) Godin, M.; Tabard-Cossa, V.; Miyahara, Y.; Monga, T.; Williams, P. J.; Beaulieu, L. Y.; Lennox, R. B.; Grutter, P. Cantilever-Based Sensing: The Origin of Surface Stress and Optimization Strategies. *Nanotechnology* **2010**, *21*, 075501.
(11) Yang, T.; Li, X.; Chen, Y.; Lee, D.-W.; Zuo, G. Adsorption Induced Surface-Stress Sensing Signal Originating from Both Vertical Interface Effects and Intermolecular Lateral Interactions. *Analyst* **2011**, *136*, 5261−5269.
(12) Halabieh, R. H. E.; Mermut, O.; Barrett, C. J. Using Light to Control Physical Properties of Polymers and Surfaces with Azobenzene Chromophores *. *Pure Appl. Chem.* **2004**, *76*, 1445−1465.
(13) Ercole, F.; Davis, T. P.; Evans, R. A. Photo-Responsive Systems and Biomaterials: Photochromic Polymers, Light-Triggered Self-Assembly, Surface Modification, Fluorescence Modulation and Beyond. *Polym. Chem.* **2010**, *1*, 37−54.
(14) Wang, R.; Jiang, L.; Iyoda, T.; Tryk, D. A.; Hashimoto, K.; Fujishima, A. Investigation of the Surface Morphology and Photo-

isomerization of an Azobenzene-Containing Ultrathin Film. *Langmuir* **1996**, *12*, 2052−2057.
(15) Ray, S. G.; Cohen, H.; Naaman, R.; Liu, H.; Waldeck, D. H. Organization-Induced Charge Redistribution in Self-Assembled Organic Monolayers on Gold. *J. Phys. Chem. B* **2005**, *109*, 14064−14073.
(16) Alloway, D. M.; Hofmann, M.; Smith, D. L.; Gruhn, N. E.; Graham, A. L.; Colorado, R.; Wysocki, V. H.; Lee, T. R.; Lee, P. A.; Armstrong, N. R. Interface Dipoles Arising from Self-Assembled Monolayers on Gold: UV−Photoemission Studies of Alkanethiols and Partially Fluorinated Alkanethiols. *J. Phys. Chem. B* **2003**, *107*, 11690−11699.
(17) Andreoni, W.; Curioni, A.; Grönbeck, H. Density Functional Theory Approach to Thiols and Disulfides on Gold: Au(111) Surface and Clusters. *Int. J. Quantum Chem.* **2000**, *80*, 598−608.
(18) Sellers, H.; Ulman, A.; Shnidman, Y.; Eilers, J. E. Structure and Binding of Alkanethiolates on Gold and Silver Surfaces: Implications for Self-Assembled Monolayers. *J. Am. Chem. Soc.* **1993**, *115*, 9389−9401.
(19) Das, B.; Abe, S. Molecular Switch on a Metal Surface. *J. Phys. Chem. B* **2006**, *110*, 4247−4255.
(20) Nagahiro, T.; Akiyama, H.; Hara, M.; Tamada, K. Photoisomerization of Azobenzene Containing Self-Assembled Monolayers Investigated by Kelvin Probe Work Function Measurements. *J. Electron Spectrosc. Relat. Phenom.* **2009**, *172*, 128−133.
(21) Tamada, K.; Akiyama, H.; Wei, T. X. Photoisomerization Reaction of Unsymmetrical Azobenzene Disulfide Self-Assembled Monolayers Studied by Surface Plasmon Spectroscopy: Influences of Side Chain Length and Contacting Medium. *Langmuir* **2002**, *18*, 5239−5246.
(22) Klajn, R. Immobilized Azobenzenes for the Construction of Photoresponsive Materials. *Pure Appl. Chem.* **2010**, *82*, 2247−2279.
(23) Fang, G.; Koral, N.; Zhu, C.; Yi, Y.; Glaser, M. A.; Maclennan, J. E.; Clark, N. A.; Korblova, E. D.; Walba, D. M. Effect of Concentration on the Photo-Orientation and Relaxation Dynamics of Self-Assembled Monolayers of Mixtures of an Azobenzene-Based Triethoxysilane with Octyltriethoxysilane. *Langmuir* **2011**, *27*, 3336−3342.
(24) Yi, Y.; Farrow, M. J.; Korblova, E.; Walba, D. M.; Furtak, T. E. High-Sensitivity Aminoazobenzene Chemisorbed Monolayers for Photoalignment of Liquid Crystals. *Langmuir* **2009**, *25*, 997−1003.
(25) Zhao, Y.; Ikeda, T. *Smart Light-Responsive Materials: Azobenzene-Containing Polymers and Liquid Crystals*; Wiley: Hoboken, NJ, 2009.
(26) Carpino, L. A.; Xia, J.; Zhang, C.; El-Faham, A. Organophosphorus and Nitro-Substituted Sulfonate Esters of 1-Hydroxy-7-azabenzotriazole as Highly Efficient Fast-Acting Peptide Coupling Reagents†. *J. Org. Chem.* **2003**, *69*, 62−71.
(27) Scott, A. F.; Gray-Munro, J. E.; Shepherd, J. L. Influence of Coating Bath Chemistry on the Deposition of 3-Mercaptopropyl Trimethoxysilane Films Deposited on Magnesium Alloy. *J. Colloid Interface Sci.* **2010**, *343*, 474−483.
(28) Ulman, A. Formation and Structure of Self-Assembled Monolayers. *Chem. Rev.* **1996**, *96*, 1533−1554.
(29) Taqatqa, O.; Attar, H. A. Spectroscopic Ellipsometry Investigation of Azo Dye and Azo Dye Doped Polymer. *Eur. Phys. J. Appl. Phys.* **2007**, *37*, 61−64.
(30) Morita, M.; Ohmi, T.; Hasegawa, E.; Kawakami, M.; Ohwada, M. Growth of Native Oxide on a Silicon Surface. *J. Appl. Phys.* **1990**, *68*, 1272−1281.
(31) Moulder, J. F. S.; Stickle, W. F.; Sobol, P. E.; Bomben, K. D. *Handbook of X-ray Photoelectron Spectroscopy*; Perkin Elmer: Eden Praire: MN, 1992.
(32) Higgins, M. J.; Proksch, R.; Sader, J. E.; Polcik, M.; Endoo, S. M.; Cleveland, J. P.; Jarvis, S. P. Noninvasive Determination of Optical Lever Sensitivity in Atomic Force Microscopy. *Rev. Sci. Instrum.* **2006**, *77*, 013701−5.
(33) Barrett, C.; Natansohn, A.; Rochod, P. Cis−Trans Thermal Isomerization Rates of Bound and Doped Azobenzenes in a Series of Polymers. *Chem. Mater.* **1995**, *7*, 899−903.
(34) Rau, H.; Yu-Quan, S. Photoisomerization of Sterically Hindered Azobenzenes. *J. Photochem. Photobiol. A: Chem.* **1988**, *42*, 321−327.
(35) Barrett, C. J.; Mamiya, J.-i.; Yager, K. G.; Ikeda, T. Photo-Mechanical Effects in Azobenzene-Containing Soft Materials. *Soft Mater* **2007**, *3*, 1249−1249.
(36) Maboudian, R. Self-Assembled Monolayers As Anti-Stiction Coatings for MEMS: Characteristics and Recent Developments. *Sens. Actuators, A* **2000**, *82*, 219−223.
(37) Yi, Y.; Fang, G.; Maclennan, J. E.; Clark, N. A.; Dahdah, J.; Furtak, T. E.; Kim, K.; Farrow, M. J.; Korblova, E.; Walba, D. M. Dynamics of Cis Isomers in Highly Sensitive Amino-Azobenzene Monolayers: The Effect of Slow Relaxation on Photo-Induced Anisotropy. *J. Appl. Phys.* **2011**, *109*, 103521−5.
(38) Fang, G. J.; Maclennan, J. E.; Yi, Y.; Glaser, M. A.; Farrow, M.; Korblova, E.; Walba, D. M.; Furtak, T. E.; Clark, N. A. Athermal Photofluidization of Glasses. *Nat Commun.* **2013**, *4*, 1521.
(39) Palik, E. D. *Hanbook of Optical Constants of Solid*; Academic Press: Orlando Florida, 1998.
(40) Watanabe, H.; Yamada, N.; Okaji, M. Linear Thermal Expansion Coefficient of Silicon from 293 to 1000 K. *Int. J. Thermophys.* **2004**, *25*, 221−236.
(41) Lide, D. R. *CRC Handbook of Chemistry and Physics*, 88th ed.; Taylor and Francis Group: Oxford, UK, 2008.
(42) Kristensen, E. M. E.; Nederberg, F.; Rensmo, H.; Bowden, T.; Hilborn, J.; Siegbahn, H. Photoelectron Spectroscopy Studies of the Functionalization of a Silicon Surface with a Phosphorylcholine-Terminated Polymer Grafted onto (3-Aminopropyl)trimethoxysilane. *Langmuir* **2006**, *22*, 9651−9657.
(43) Janssen, G. C. A. M.; Abdalla, M. M.; van Keulen, F.; Pujada, B. R.; van Venrooy, B. Celebrating the 100th anniversary of the Stoney Equation for Film Stress: Developments from Polycrystalline Steel Strips to Single Crystal Silicon Wafers. *Thin Solid Films* **2009**, *517*, 1858−1867.
(44) Hopcroft, M. A.; Nix, W. D.; Kenny, T. W. What is the Young's Modulus of Silicon? *J. Microelectromech. Syst.* **2010**, *19*, 229−238.